Bottom up approach toward prediction of effective thermophysical properties of carbon-based nanofluids

Bottom up approach towards prediction of effective thermophysical properties of carbon-based nanofluids

Matteo Fasano[1,*], Masoud Bozorg Bigdeli[2]

[1] *Politecnico di Torino, Energy Department, Corso Duca degli Abruzzi, 24, 10129 Turin, Italy*
[2] *University of Alberta, Department of Mechanical Engineering, 9211-116 Street NW, Edmonton Alberta, Canada*

* Corresponding Author. Email: matteo.fasano@polito.it; Mailing address: Politecnico di Torino, Energy Department, Corso Duca degli Abruzzi, 24, 10129 Turin, Italy; Tel. 0039-011-0904435; Fax. 0039-011-0904499

Abstract

Carbon-based nanofluids, mainly suspensions of carbon nanotubes or graphene sheets in water, are typically characterized by superior thermal and optical properties. However, their multiscale nature is slowing down the investigation of optimal geometrical, chemical, and physical nanoscale parameters for enhancing the thermal conductivity while limiting the viscosity increase at the same time. In this work, a bottom up approach is developed to systematically explore the thermophysical properties of carbon-based nanofluids with different characteristics. Prandtl number is suggested as the most adequate parameter for evaluating the best compromise between thermal conductivity and viscosity increases. By comparing the Prandtl number of nanofluids with different characteristics, promising overall performances (that is, nanofluid/base fluid Prandtl number ratios equal to 0.7) are observed for semidilute (volume fraction ≤ 0.004) aqueous suspensions of carbon nanoparticles with extreme aspect ratios (larger than 100 for nanotubes, smaller than 0.01 for nanoplatelets) and limited defects concentrations (less than 5%). The bottom up approach discussed in this work may ease a more systematic exploration of carbon-based nanofluids for thermal applications, especially solar ones.

The Version of Record of this manuscript has been published and is available in *Heat Transfer Engineering*, 24 October 2017, https://doi.org/10.1080/01457632.2017.1384283

Introduction

The advent of nanotechnology has offered novel possibilities to extend the performance limit of conventional energy and biomedical systems [1-12]. In particular, the heat transfer enhancement of heat exchangers by using working fluids with larger thermal conductivities has received increased attention over the past twenty years [13]. To this purpose, nano-sized particles with high thermal conductivity can be dispersed into conventional heat transfer fluids, such as oil or water. Such nanoparticle suspensions are also known as nanofluids [14-16]. Several studies have been carried out on the thermophysical properties of nanofluids, namely on their viscosity (μ), density (ρ), specific heat capacity (c_p) and thermal conductivity (λ). Nanofluids made of oxide, ceramic or carbon-based particles generally have thermal conductivities, densities, and viscosities larger than the ones of traditional base fluids. It is also well established that λ, ρ and μ increase with the volume concentration (ϕ) of nanoparticles. On the other side, specific heat capacity of nanofluids is lower than base fluid, and it decreases with increasing ϕ [17].

For dilute and semidilute suspensions of nanoparticles, thermal conductivity increases in accordance with predictions of effective medium theories (EMTs). On the other hand, for higher concentrations, λ goes beyond predictions of EMTs models, mainly because of the formation of thermal percolation paths within the fluid induced by nanoparticles aggregation [18-20].

Carbon-based particles – graphene and carbon nanotubes in particular – have received widespread attention because of their superior thermal, electrical, optical, and mechanical properties, if compared to ceramic and metallic particles. Carbon-based nanofluids (CNFs) are prepared by dispersing carbon-based nanoparticles in base fluids,

such as water, engine oil or ethylene glycol [21, 22]. Addition of surfactants or particle surface functionalizations may be required for a stable suspension. The research on CNFs is driven by their potential in automotive, biomedical and mostly solar applications [23].

Hordy *et al.* [23] studied the optical properties and stability of suspensions of plasma-functionalized multi-walled carbon nanotubes (MWCNTs) in water, Therminol® VP-1, ethylene glycol (EG) and propylene glycol (PG) for direct solar absorption. The stored energy fraction, namely the fraction of solar energy absorbed by the fluid for a given penetration distance, was evaluated for the presented MWCNT nanofluids, proving the improvement of the energy storage ability for the considered CNFs. Moreover, the long-term stability of the nanofluids at room temperature over a period of 8 months was examined: the EG- and PG-based nanofluids remained almost stable over this period, while a gradual decrease of concentration was observed for the water-based nanofluids. In addition, the high temperature stabilities of these nanofluids were investigated, and no change was evidenced for water- and glycol-based nanofluids after heating up to 85 and 170°C, respectively. These nanofluids can serve as both heat transfer fluids and volumetric solar collectors. Such findings lead to enhancements in efficiencies of solar thermal devices, while reducing the associated costs.

Ding *et al.* [24] measured the effective thermal conductivity, viscosity and heat transfer coefficient of water-based suspensions of carbon nanotubes (CNTs), with gum arabic as dispersant. They observed that λ increases with increasing temperature and volume concentration of nanotubes. The viscosity also increased with ϕ, while decreased with larger temperatures. Ding *et al.* [24] realized that the convective heat transfer

coefficient (h) depends on flow regime, pH and concentration of carbon nanotubes. The measured h was significantly improved with respect to the base fluid (up to 350%).

On the other hand, recent studies on carbon-based nanofluids have revealed the importance of nanoparticle characteristics, *i.e.* shape, size, surface functionalization and presence of defects, on the effective performances of CNFs.

As for the effect of surface functionalization, Abbasi *et al.* [25] showed that the presence of functional groups promotes the dispersion quality of MWCNTs in a hybrid nanofluid of carbon nanotubes/gamma alumina particles. They discuss that this is due to the reduction of van der Waals interactions among MWCNTs. However, the introduction of functional groups should be controlled, since it leads to the generation of defects on the surface and thus decrease in the thermal conductivity of MWCNTs.

Aravind and Ramaprabhu [26] investigated the thermal conductivity of water- and EG-based graphene and hybrid graphene-MWCNT nanofluids. The hybrid nanofluid exhibited higher thermal conductivities. In fact, due to their high aspect ratios, CNTs have the potential to develop chains of an interconnected network. Such network acts as a conducting path, hence hybrid nanofluids made of both graphene (oblate) and MWCNT (prolate) with high aspect ratios may experience higher thermal conductivity values.

This brief literature review proves that multiple factors account for the effective thermophysical properties of nanofluids. Hence, the broad variety of combinations of geometrical and physical parameters makes it difficult to choose the optimal characteristics of the nanofluid to be synthesized. Therefore, a computational-driven approach would be beneficial in the parameters selection, in order to find an optimal compromise between thermophysical properties of nanofluids.

In this work, a bottom up methodology (*i.e.*, from nanoscale characteristics to effective materials properties) to quickly explore the overall thermophysical properties of nanofluids is first introduced. Then, a detailed sensitivity analysis of the effect of nanoscale characteristics of carbon nanoparticles on the resulting thermophysical properties of nanofluids is carried out. In particular, different geometrical (size, shape) and chemical (material, defectiveness) characteristics of CNTs and graphene nanoplatelets (GNPs) suspended in water are considered. The Prandtl number decrease induced by nanoparticle insertion in a base fluid ($\mathrm{Pr}/\mathrm{Pr}_0$) is considered as the most comprehensive performance index for the thermophysical properties of nanofluids for thermal applications, where both enhanced thermal conductivity and limited viscosity are generally required.

The article is structured as follows: the bottom up methodology adopted for evaluating the thermophysical properties of nanofluids is first presented; this approach is then applied to suspensions of alumina nanoparticles, carbon nanotubes or graphene nanoplatelets in water, to explore the relation between their nanoscale characteristics and effective properties; finally, conclusions and perspectives are drawn.

Methods

Due to their multiscale nature, the effective thermophysical properties of nanofluids are strongly affected by nanoscale phenomena. Several models have been introduced to predict macroscale properties of nanofluids starting from the geometrical, physical and chemical characteristics of their constituents, mainly nanoparticles, surfactants and base fluid [27]. In a bottom up approach, the effective properties of nanostructured materials are computed by only relying on the nanoscale characteristics of each constituent. In this study,

the following procedure is considered for determining the thermophysical properties of nanofluids based on carbon nanotubes or nanoplatelets:

1. nanoscale thermal conductivity of carbon nanoparticles is taken from experimental/computational evidences in the literature, according to different shape, size and defect concentration of nanoparticles;
2. effective thermal conductivity of nanofluid is estimated by effective medium theory, by considering the nanoscale thermal conductivity of nanoparticles obtained in the previous step;
3. viscosity of nanofluid is estimated from semi-empirical correlations validated in the literature, according to different shape, size and volume fraction of nanoparticles;
4. specific heat capacity of nanofluid is estimated from mixing rule, according to different volume fraction of nanoparticles;
5. Prandtl number of nanofluid is finally computed from the thermophysical properties estimated in previous steps.

After two decades of investigations, it is now accepted that the thermal properties of well dispersed nanoparticle suspensions can be described by adaptations of classical effective medium theory [28]. On the other hand, nanoparticles aggregation may lead to highly conductive percolation paths, which enhance the effective thermal conductivity of nanofluids beyond effective medium theory predictions [29, 30]. Therefore, the effective thermal conductivity of nanofluids can be computed by expressions derived from classical effective medium theory only under dilute and semidilute conditions (*i.e.*, low volume fractions of nanoparticles in the base fluid), where clustering phenomena are substantially

avoided. Under this hypothesis, Nan *et al.* [31] generalized the Maxwell's effective medium theory to include the effect of particle shape and finite interfacial resistance:

$$\frac{\lambda}{\lambda_0} = \frac{3 + \phi[2\beta_{11}(1 - L_{11}) + \beta_{33}(1 - L_{33})]}{3 - \phi(2\beta_{11}L_{11} + \beta_{33}L_{33})} \tag{1}$$

where λ and λ_0 refer to the thermal conductivity of nanofluid and base fluid, respectively. In case of prolate and oblate particles, the principal axes are $a_{11} = a_{22} < a_{33}$, therefore $p = a_{33}/a_{11}$ and parameters in Equation (1) take the form:

$$L_{11} = \frac{p^2}{2(p^2 - 1)} - \frac{p}{2(p^2 - 1)^{\frac{3}{2}}}\cosh^{-1}p$$

$$L_{33} = 1 - 2L_{11}$$

$$\beta_{ii} = \frac{\lambda_{ii}^c - \lambda_0}{\lambda_0 + L_{ii}(\lambda_{ii}^c - \lambda_0)}$$

being

$$\lambda_{ii}^c = \frac{\lambda_p}{1 + \gamma L_{ii}\lambda_p/\lambda_0}$$

$$\gamma = \frac{\left(2 + \frac{1}{p}\right) R_k \lambda_0}{(a_{11}/2)}$$

R_k the Kapitza resistance at the solid-liquid interface and λ_p the thermal conductivity of particle. Equation (1) is in agreement with experiments for a broad variety of nanofluids with less than 18% error [28]; however, this theory is bounded by linear aggregation models at extreme aspect ratios [19, 29, 30]. Nevertheless, here we study semidilute suspensions of nanoparticles ($\phi \leq 0.004$), where aggregation probability is low.

On the other side, a general enhancement in nanofluids viscosity has been reported with increasing ϕ, and several theoretical or empirical models have been suggested to interpret experimental results [32]. An analytical relation between the viscosity of colloidal

suspensions and their volume fraction (with $\phi \leq 0.02$) has been introduced by Einstein in 1906 [33]:

$$\frac{\mu}{\mu_0} = 1 + B\phi \tag{2}$$

being μ and μ_0 the dynamic viscosities of suspension and base fluid, whereas $B = 2.5$ the intrinsic viscosity (also known as "Einstein coefficient") in the first formulation by Einstein. Notwithstanding extensive investigations on nanofluids, this B value has not been incontrovertibly confirmed by experiments, where optimal intrinsic viscosities span in the range $1.5 < B < 5$, being for instance affected by particle material, shape, interaction and aggregation [34].

Instead, specific heat capacity of nanofluids can be accurately predicted by a simple mixing rule, namely

$$c_p = (1 - \phi)c_{p,0} + \phi c_{p,p} \tag{3}$$

where c_p, $c_{p,0}$ and $c_{p,p}$ are the specific heat capacities of nanofluid, base fluid and nanoparticles, respectively [17].

The Prandtl number of a nanofluid can be finally computed as

$$\mathrm{Pr} = \frac{\mu c_p}{\lambda} \tag{4}$$

therefore allowing to compare the typical enhancements in both thermal conductivity and viscosity due to nanoparticles insertion in a base fluid. The Prandtl number of nanofluid (Pr) can be then compared to the Prandtl number of base fluid ($\mathrm{Pr}_0 = \frac{\mu_0 c_{p,0}}{\lambda_0}$), in order to achieve a global evaluation of the thermophysical properties of nanofluids with respect to the corresponding base fluids.

Results

Alumina-based nanofluids: a case study

As evident in Equation (1), a critical parameter in determining thermal properties of nanofluids is nanoparticle geometry. To explore this effect, we first consider suspensions of alumina nanoparticles in water, as a simple case study. In fact, alumina nanoparticles can be synthesized in a broad variety of sizes (from 2 to 300 nm radii) and shapes (spheres, cylinders or platelets) [35-38].

By considering the thermal conductivity of alumina nanoparticles ($\lambda_p = 35$ W/mK [28]), de-ionized water at ambient temperature ($\lambda_0 = 0.61$ W/mK) and a typical value for the Kapitza resistance between solid hydrophilic surfaces and water ($R_k = 10^{-8}$ m^{2}K/W [39, 40]), Equation (1) allows to predict the thermal conductivity of alumina-based nanofluids with different size ($5\text{ nm} \leq a_{11} \leq 200\text{ nm};\ 5\text{ nm} \leq a_{33} \leq 200\text{ nm}$) and aspect ratio ($0.025 \leq p \leq 40$) of the solvated nanoparticles. Figure 1a reports the resulting thermal conductivity enhancement (λ/λ_0) at a typical particle volume fraction of $\phi = 0.01$, and it allows to highlight some relations between nanoscale characteristics of nanofluids and their effective thermal properties. First, the insertion of alumina nanoparticles induces a general increase in thermal conductivity with respect to base fluid ($1.00 < \lambda/\lambda_0 \leq 1.10$) [28]; second, at fixed ϕ and under well-dispersed conditions, the thermal conductivity enhancement is proportional to nanoparticle size (from $\lambda/\lambda_0 \cong 1$ at $a_{11} = a_{33} = 5$ nm, to $\lambda/\lambda_0 \cong 1.02$ at $a_{11} = a_{33} = 200$ nm) [41]; third, extreme aspect ratios lead to the largest thermal conductivity enhancements (up to $\lambda/\lambda_0 = 1.10$), especially at large particle sizes [40]. Note that, while the latter relation with aspect ratio finds good agreement with several experiments [36, 37, 40, 42], the former direct

proportionality between particle size and thermal conductivity enhancement is still controversial in the literature, being strongly related to the adopted synthesis procedure, pH, surfactants and additives, which may lead to totally different particle aggregation phenomena and thus λ/λ_0 [17, 35]. In Fig. 1b, Equation (1) is instead applied to alumina-based nanofluids with a larger particle volume fraction, namely $\phi = 0.02$. Results show a direct proportionality between λ/λ_0 and ϕ, while previous considerations still hold with generally larger thermal conductivity enhancements (up to $\lambda/\lambda_0 = 1.20$ at $a_{11} = 5$ nm and $a_{33} = 200$ nm). Furthermore, Fig. 1b allows to better appreciate the larger thermal conductivity increases given by prolate nanoparticles ($p > 1$, up to $\lambda/\lambda_0 = 1.20$) with respect to oblate ($p < 1$, up to $\lambda/\lambda_0 = 1.14$) ones.

Hence, prolate (e.g. rods or nanotubes) or oblate (e.g. platelets) nanoparticles should be preferred in heat transfer applications, because of the particularly enhanced thermal conductivity of resulting nanofluids (see Fig. 1c) [42]. In the following analyses, nanofluids containing carbon nanoparticles with extreme aspect ratios are therefore preferentially investigated.

Thermal conductivity of carbon nanoparticles

Carbon-based nanofluids have attracted an exponentially increasing attention in the last few years, because of their superior thermal transport and optical properties, which make them ideal candidates for solar applications [43-53]. Here, thanks to a bottom up approach, Equations (1) to (4) are adopted to explore the effect of geometrical (size, length) and chemical (material, defects) characteristics of nanoparticles on the overall thermophysical properties of nanofluids.

The following analyses are focused on nanoparticles intrinsically characterized by extreme aspect ratios and high thermal conductivities, namely: (i) carbon nanotubes, which can be considered as prolate particles with $p = L/D \gg 1$ (Fig. 2a); (ii) graphene nanoplatelets, which have oblate shapes and $p = T/L_x = T/L_y \ll 1$ (Fig. 2b).

First, the size of a pristine carbon nanoparticle strongly influences its thermal conductivity. On the one hand, both experimental and numerical studies suggest that $\lambda \sim L^{\alpha}$ in CNTs, where best fitted values of α have been found in the range $0.2 - 0.8$ [4, 54-56]. In fact, increased nanotube sizes are responsible of additional vibrational modes with longer wavelengths, which introduce further pathways to conductive heat transfer by phonons. For example, Fig. 3a reports the thermal conductivities of pristine CNTs (λ_{ref}) numerically computed by Alaghemandi *et al.* [54] with different lengths and diameters (black dots). While diameter appears to have little or no influence on λ_{ref}, the nanotube length significantly alters it, spanning from $40\ \mathrm{W/mK}$ ($L = 5$ nm) to $590\ \mathrm{W/mK}$ ($L = 350$ nm). While Alaghemandi *et al.* [54] suggest that $\alpha = 0.77$ for $L = 5 - 25$ nm and $\alpha = 0.54$ for $L = 100 - 350$ nm, here the numerical results reported in [54] have been empirically fitted ($R^2 = 0.99$, dashed line in Fig. 3a) by $\lambda_{ref} = k_1 L^{\alpha} + k_2$ ($k_1 = 77\ \mathrm{W/mK}$; $\alpha = 0.37$; $k_2 = -100\ \mathrm{W/mK}$; L expressed in nm), for a continuous representation of $\lambda_{ref} - L$ relation in the considered lengths range. On the other hand, similar considerations can be argued for pristine graphene sheets, where the sheet size is observed to affect thermal conductivity as $\lambda \sim \ln(L)$ [57]. For example, Xu *et al.* [58] reported experimental and numerical thermal conductivities of suspended, pristine single-layer graphene, showing a logarithmic divergence of λ_{ref} with sample length (Fig. 3c, dots). Again, the results reported by Xu *et al.* [58] have been empirically fitted ($R^2 = 0.96$,

dashed line in Fig. 3c) by $\lambda_{ref} = k_3 \ln(k_4 L) + k_5$ ($k_3 = 447$ W/mK; $k_4 = 8.07 \times 10^{-2}$; $k_5 = -4.38$ W/mK; L expressed in nm). Note that Xu *et al.* [58] verified that the logarithmic relation between thermal conductivity and graphene size beyond the ballistic regime is not related to the aspect ratio (L_x/L_y, see Fig. 2b), namely is only related to the largest dimension of the graphene sheet.

Second, the thermal conductivity of pristine carbon nanoparticles obtained at lab conditions (λ_{ref}) is typically reduced by the presence of defects under operative conditions (λ_p). A broad variety of defects may be found in both CNTs and GNPs. In fact, vacancies, Stone-Wales defects, surface functionalizations or atom substitutions (doping) in carbon nanotubes or graphene sheets are observed to cause exponential-like decays of λ with their concentration, mainly because of localized phonon scattering [59-64]. As a comprehensive case for CNT's defects, Sevik *et al.* [65] systematically investigated λ_p/λ_{ref} for randomly distributed multiple defects (single and double vacancies, Stone-Wales defects) within CNTs with different length and chirality. The results obtained by Sevik *et al.* [65] are reported in Fig. 3b (dots), being accurately fitted ($R^2 = 0.99$, dashed line) by $\lambda_p/\lambda_{ref} = (k_6 + k_7 d_{\%})/(k_8 + k_9 d_{\%} + d_{\%}^2)$ ($k_6 = 0.124$; $k_7 = 0.292$; $k_8 = 0.124$; $k_9 = 2.361$), where $d_{\%}$ is the concentration of defects expressed as a percent of CNT surface. Similarly, Zhu *et al.* [66] investigated the thermal conductivity reduction induced by a broad variety of randomly distributed topological defects in graphene nanoribbons. In their work, Zhu *et al.* [66] report a significant drop in thermal conductivity with defects concentration, which eventually achieves 70% reduction at $d_{\%} \cong 5\%$ (Fig. 3d, dots). Moreover, Zhu and coworkers propose $\lambda_p/\lambda_{ref} = 1/(1 + k_{10} d_{\%})$ as best fit of their results ($k_{10} = 0.593$, dashed line in Fig. 3d).

Effective thermophysical properties of carbon-based nanofluids

CNT- and GNP-based nanofluids tested in solar applications typically adopt water as base fluid, because of both superior heat capacity and reduced environmental impact [43, 45, 46, 48-51, 67]. Hence, the generally hydrophobic surface of carbon nanoparticles should be treated by either chemical functionalization or surfactant adsorption, to increase its water affinity thus obtaining stable suspensions.

Suspensions of CNTs or GNPs in de-ionized water at ambient temperature can be then considered, while adopting $R_k = 10^{-8}\ \mathrm{m^2K/W}$ as a typical Kapitza resistance between the hydrophilic surface of nanoparticles and the polar fluid [39, 40]. Note that the bottom up methodology discussed here has rather general validity and, therefore, it could be eventually adopted to perform sensitivity analyses with base fluids different from pure water (e.g., water/ethylene glycol mixtures). Equation (1) allows a bottom up exploration of the thermal conductivity enhancement in carbon-based nanofluids as a function of particle material (CNTs; GNPs), length (CNTs with fixed 4 nm diameter and $10\ \mathrm{nm} \leq L \leq 500\ \mathrm{nm}$; GNPs with fixed 2 nm width and $10\ \mathrm{nm} \leq L \leq 2000\ \mathrm{nm}$), shape (prolate CNTs with $2.5 \leq p \leq 125$; oblate GNPs with $0.001 \leq p \leq 0.2$), defect concentration (CNTs with $0\% \leq d_{\%} \leq 1\%$; GNPs with $0\% \leq d_{\%} \leq 5\%$) and particle volume fraction ($\phi = 0.002$ or 0.004). Note that L, p, $d_{\%}$ and ϕ have been chosen to lie within the typical working conditions of nanofluids for solar applications [43, 45, 46, 48-51], while $\lambda_p = f(L, d_{\%})$ as reported in Fig. 3.

Figure 4a shows the resulting thermal conductivity enhancements (λ/λ_0) of CNT-based nanofluids at $\phi = 0.002$, whereas Fig. 4b at $\phi = 0.004$. Results indicate that defect concentration – which may depend on the synthesis technique, handling and storage

processes, and working conditions of nanofluids – dramatically alters the thermal conductivity of nanofluids with apparently identical characteristics. For example, a 1% defect concentration causes a 20% decrease in λ/λ_0, namely from $\lambda/\lambda_0 = 1.44$ to 1.13 ($\phi = 0.004$; $L = 500$ nm). Furthermore, longer CNTs show beneficial effects on thermal conductivity of nanofluid, because of both increased aspect ratio and λ_p. It is also clear that, at least in the considered range of particle volume concentrations, λ/λ_0 is directly proportional to ϕ: for instance, λ/λ_0 passes from 1.22 to 1.44 by doubling ϕ ($d_{\%} = 0\%$; $L = 500$ nm). As visible in Fig. 4c ($\phi = 0.002$) and d ($\phi = 0.004$), similar considerations can be also formulated for GNP-based nanosuspensions, even though both larger λ/λ_0 enhancements and reduced sensitivity to defect concentration can be noticed. The difference between CNT and GNP behavior can be mainly attributed to different $\lambda_p = f(L, d_{\%})$ relations (see Fig. 3), aspect ratios and considered length range. Note that the reported results lie in the typical λ/λ_0 ranges found in experimental investigations (see for example [43, 68-72] and [45, 73] for CNT and graphene-based nanofluids, respectively), where large variabilities are mainly due to the adopted synthesis protocol (*i.e.*, defects concentration, surfactants and surface functionalizations) and experimental conditions (*i.e.*, temperature and particle aggregation).

However, the enhanced thermal conductivity of nanofluids is not sufficient to evaluate their overall effectiveness in thermal applications; in fact, fluid viscosity typically increases with nanoparticle addition. Equation (2) allows estimating the viscosity increase in nanofluids with volume concentrations up to 2%, being the B parameter substantially affected by particle shape and motion (*i.e.*, prevailing orientation respect to flow direction) in a shearing fluid. Mueller *et al.* [34] estimated – both numerically and experimentally –

a relation between B, particle shape (*i.e.*, aspect ratio p) and motion: Fig. 5a reports the results for initially random orientated particles, where original data (dots) are accurately fitted ($R^2 = 0.99$) by the double exponential function $B = k_{11}\exp(k_{12}p) + k_{13}\exp(k_{14}p)$ (solid line; $k_{11} = 2.09$; $k_{12} = -0.16$; $k_{13} = 0.45$; $k_{14} = 0.65$). The previous relation allows estimating the viscosity enhancement in the carbon-based nanofluids considered in Fig. 4 with respect to base fluid ($\mu_0 = 8.51 \times 10^{-4}$ Pa s; $T = 300$ K). Here, the concentration of nanoparticle defects (e.g., vacancies, Stone-Wales, atom substitution) is assumed to have no significant effect on nanofluid viscosity. Results in Fig. 5b show that μ/μ_0 increases with ϕ and extreme aspect ratios, which depend on the particle lengths for the considered carbon nanoparticles (see Fig. 2). The viscosity enhancements in Fig. 5b range from 0.5% ($p \approx 1$ and $\phi = 0.002$) to 5% ($p > 100$ and $\phi = 0.004$) with respect to pure water. Note that the analyzed nanofluids lie under semidilute conditions, therefore the relation reported in Fig. 5a holds [34]. Results in Fig. 5b find qualitative agreement with experimental μ/μ_0 values (e.g., results reported in [69, 72] and [45, 73] for CNT and graphene-based nanofluids, respectively), where large variabilities are again due to the adopted synthesis protocols and experimental conditions.

The effect of thermal conductivity and viscosity enhancements reported in Figs. 4 and 5 can be finally compared to estimate the overall performances of the considered carbon-based nanofluids. In fact, while larger λ typically lead to beneficial effects in terms of heat transfer effectiveness, larger μ are responsible for increased pumping power and wear and tear of mechanical parts. By considering the ratio between momentum and thermal diffusivities, Prandtl number allows to compare these contrasting effects and to identify the most favorable parameters of nanofluids for thermal applications, namely the

ones minimizing Pr. In Fig. 6, the Prandtl number for the carbon-based nanofluids discussed in Figs. 4 and 5 are computed by Equations (1) – (4) , being $c_p = 700$ J/kg K the typical specific heat capacity of carbon nanoparticles at ambient temperatures [74-76]. In general, results show that larger ϕ and L (thus p) are beneficial to $\mathrm{Pr}/\mathrm{Pr}_0$ reduction, whereas $d_{\%}$ has a detrimental effect. For example, nanofluids made of GNPs can be analyzed ($\phi = 0.002$ in Fig. 6c; $\phi = 0.004$ in Fig. 6d): while $\mathrm{Pr}/\mathrm{Pr}_0$ is larger than one with short particles and thus low aspect ratios, $\mathrm{Pr}/\mathrm{Pr}_0$ shows up to 18% ($\phi = 0.002$) or 30% ($\phi = 0.002$) reduction with $L = 2000$ nm. Therefore, the smaller is $\mathrm{Pr}/\mathrm{Pr}_0$the better is the nanofluid performance in heat transfer (or solar) applications, being $\mathrm{Pr}/\mathrm{Pr}_0 = 0.7$ the lowest value achieved in the considered range of geometrical and chemical parameters. In summary, these results highlight promising overall performances (*i.e.*, $\mathrm{Pr}/\mathrm{Pr}_0 < 1$) for nanofluids made of oblate (e.g. nanoplatelets) or prolate (e.g. nanotubes) carbon-based nanoparticles in thermal applications, at least for extreme aspect ratios ($p > 100$ or $p < 0.01$) and semidilute conditions ($\phi \leq 0.004$).

The bottom up approach to explore the thermophysical properties of nanofluids of interest for thermal applications can be finally compared with some recent experimental works in the literature. For example, Sandhu and Gangacharyulu [77] studied the experimental thermophysical properties of nanofluids made of multi-walled carbon nanotubes suspended in water. In their experiments, they tested nanotubes with 3–8 μm length and 10–20 nm outer diameter, which were characterized by 99% purity. Carbon nanotubes were then dispersed into water (0.1% volume fraction), and the effective thermal conductivity, density, and viscosity of the resulting nanofluid measured. Results show that the Prandtl number of nanofluid is reduced with respect to the base fluid, that is $\mathrm{Pr}/\mathrm{Pr}_0 =$

0.90. This is in good accordance with the bottom up approach discussed so far, which estimates an average value of $\mathrm{Pr}/\mathrm{Pr}_0 = 0.92$ (2.7% discrepancy). Xing *et al.* [78], instead, investigated by experiments the thermophysical properties of single-walled carbon nanotubes (5–30 μm length; 1–2 nm outer diameter; >90% purity) in water. A water-based nanofluid with 0.1% mass fraction of nanotubes revealed an enhanced Prandtl number with respect to the base fluid, namely $\mathrm{Pr}/\mathrm{Pr}_0 = 1.03$. Also in this case, the bottom up approach presents a good approximation of the experimental results, with a predicted value of $\mathrm{Pr}/\mathrm{Pr}_0 = 1.12$ (8.9% discrepancy). Note that the model predictions lie within a typical 10% overall experimental error and, therefore, a good reliability of the bottom up approach is demonstrated, at least for a preliminary general assessment of the most interesting characteristics of semidilute nanofluids for thermal applications. The accuracy of the bottom up approach could be eventually improved by a more mechanistic derivation of the Kapitza resistance at the fiber-fluid interface [79], which is only taken as an average value [39] in the current implementation of the approach.

Conclusions

Carbon-based nanofluids have been recently indicated as the core element of next generation solar absorbers, because of their superior thermal and optical properties. However, the multiscale nature of such suspensions of nanoparticles introduces a large set of geometrical, chemical, and physical nanoscale parameters affecting their effective properties, which actually slows down the exploration of optimal nanofluids characteristics in thermal applications.

In this work, a bottom up approach is suggested to systematically explore the thermophysical properties of carbon-based nanofluids with different geometrical, chemical, and physical characteristics. Starting from experimentally validated physical relations between nanoscale and macroscale properties of nanofluids, our aim is to look for the combinations of nanoparticles' characteristics that provide the largest decrease in the Prandtl number of nanofluid, namely the best compromise between thermal conductivity enhancement and limited viscosity increase. Therefore, the variations in nanofluids thermal conductivity, viscosity and specific heat capacity induced by altering the nanoparticles material, shape and defectiveness are here investigated. Results indicate promising overall performances (*i.e.*, up to $\mathrm{Pr}/\mathrm{Pr}_0 \cong 0.7$) for nanofluids made of carbon nanoparticles with extreme aspect ratios (e.g., either nanoplatelets or nanotubes) and limited defects concentrations.

The reported results hold under dilute and semidilute conditions ($\phi \leq 0.004$), whereas the effect of particle aggregation and thus the creation of percolation paths favoring heat conduction should be further explored in successive works. Moreover, both particle aggregation and heat conduction at the solid-liquid interface may be altered by surfactants, such as sodium dodecyl sulphate [47] or Triton X-100 [51], which are typically adopted to improve the suspension stability and should be properly taken into account in predicting the Prandtl number of nanofluids. However, the bottom up approach to nanofluids properties discussed in this work would still be an adequate way to systematically explore the most interesting set of nanoscale parameters in colloidal suspensions for a broad variety of engineering and biomedical applications, with special focus on solar applications.

Acknowledgment

Authors thank the Politecnico di Torino's DAUIN high-performance computing initiative for the availability of high-performance computing resources and support. Authors would like to acknowledge the NANO-BRIDGE (PRIN 2012, grant number 2012LHPSJC), the GRAPHENE@POLITO (Graphene Flagship) and the NANOSTEP (Fondazione CRT, Torino) projects.

Nomenclature

a_{ij}	Principal axis of ellipsoidal particle	$[m]$
B	Intrinsic viscosity	$[-]$
CNF	Carbon-based nanofluids	
CNT	Carbon nanotube	
c_p	Specific heat capacity	$[J\ kg^{-1}K^{-1}]$
$d_{\%}$	Percent defect concentration	[%]
D	Diameter	$[m]$
EG	Ethylene glycol	
EMT	Effective medium theory	
GNP	Graphene Nanoplatelet	
h	Convective heat transfer coefficient	$[W\ m^{-2}K^{-1}]$
L	Length	$[m]$

MWCNT	Multi-walled carbon nanotube	
N	Number density	$[m^{-3}]$
p	Aspect ratio	$[-]$
PG	Propylene glycol	
Pr	Prandtl number	$[-]$
R_k	Kapitza resistance	$[m^2\ K\ W^{-1}]$
R^2	Coefficient of determination	$[-]$
T	Thickness	$[m]$

Greek symbols

λ	Thermal conductivity	$[W\ m^{-1}K^{-1}]$
μ	Dynamic viscosity	$[Pa\ s]$
ϕ	Volume fraction	$[-]$
ρ	Density	$[kg\ m^{-3}]$

Subscripts

p	Particle
ref	Reference, pristine nanoparticle
x, y	Cartesian coordinates
0	Base fluid

Superscript

α Power law exponent

References

[1] Moniz, E.J., and Garcia-Martinez, J., *Nanotechnology for the energy challenge*. Weinheim, Germany: John Wiley & Sons, 2010

[2] Fasano, M., Borri, D., Chiavazzo, E., and Asinari, P., Protocols for atomistic modeling of water uptake into zeolite crystals for thermal storage and other applications, *Applied Thermal Engineering*, vol. 101: pp. 762-769, 2016.

[3] Fasano, M., Chiavazzo, E., and Asinari, P., Water transport control in carbon nanotube arrays, *Nanoscale research letters*, vol. 9: 1, pp. 1-8, 2014.

[4] Fasano, M., Bigdeli, M.B., Sereshk, M.R.V., Chiavazzo, E., and Asinari, P., Thermal transmittance of carbon nanotube networks: guidelines for novel thermal storage systems and polymeric material of thermal interest, *Renewable and Sustainable Energy Reviews*, vol. 41: pp. 1028-1036, 2015.

[5] Chiavazzo, E., and Asinari, P., Reconstruction and modeling of 3D percolation networks of carbon fillers in a polymer matrix, *International Journal of Thermal Sciences*, vol. 49: 12, pp. 2272-2281, 2010.

[6] Chiavazzo, E., and Asinari, P., Enhancing surface heat transfer by carbon nanofins: towards an alternative to nanofluids?, *Nanoscale research letters*, vol. 6: 1, pp. 1-13, 2011.

[7] Chiavazzo, E., Fasano, M., Asinari, P., and Decuzzi, P., Scaling behaviour for the water transport in nanoconfined geometries, *Nature communications*, vol. 5: 3565, pp. 1-11, 2014.

[8] Gizzatov, A., Key, J., Aryal, S., Ananta, J., Cervadoro, A., Palange, A.L., Fasano, M., Stigliano, C., Zhong, M., Di Mascolo, D., Guven, A., Chiavazzo, E., Asinari, P., Liu, X., Ferrari, M., Wilson, L.J., and Decuzzi, P., Hierarchically structured magnetic nanoconstructs with enhanced relaxivity and cooperative tumor accumulation, *Advanced functional materials*, vol. 24: 29, pp. 4584-4594, 2014.

[9] Cardellini, A., Fasano, M., Chiavazzo, E., and Asinari, P., Mass transport phenomena at solid-liquid nanoscale interface in biomedical applications, in *VI International Conference on Computational Methods for Coupled Problems in Science and Engineering COUPLED PROBLEMS 2015*, International Center for Numerical Methods in Engineering (CIMNE), pp. 593-604, Venice, Italy May 18-20, 2015.

[10] Cardellini, A., Fasano, M., Chiavazzo, E., and Asinari, P., Interfacial water thickness at inorganic nanoconstructs and biomolecules: Size matters, *Physics Letters A*, vol. 380: 20, pp. 1735-1740, 2016.

[11] Chougule, S.S., and Sahu, S.K., Comparative study of cooling performance of automobile radiator using Al2O3-water and carbon nanotube-water nanofluid, *Journal of Nanotechnology in Engineering and Medicine*, vol. 5: 1, pp. 010901/1-010901/7, 2014.

[12] Fasano, M., Humplik, T., Bevilacqua, A., Tsapatsis, M., Chiavazzo, E., Wang, E.N., and Asinari, P., Interplay between hydrophilicity and surface barriers on water transport in zeolite membranes, *Nature Communications*, vol. 7: 12762, pp. 1-8, 2016.

[13] Taylor, R., Coulombe, S., Otanicar, T., Phelan, P., Gunawan, A., Lv, W., Rosengarten, G., Prasher, R., and Tyagi, H., Small particles, big impacts: a review

of the diverse applications of nanofluids, *Journal of Applied Physics*, vol. 113: 1, pp. 011301/1-011301/18, 2013.

[14] Keblinski, P., Eastman, J.A., and Cahill, D.G., Nanofluids for thermal transport, *Materials today*, vol. 8: 6, pp. 36-44, 2005.

[15] Das, S.K., Choi, S.U., and Patel, H.E., Heat transfer in nanofluids—a review, *Heat transfer engineering*, vol. 27: 10, pp. 3-19, 2006.

[16] Tascini, A.S., Armstrong, J., Chiavazzo, E., Fasano, M., Asinari, P., and Bresme, F., Thermal transport across nanoparticle–fluid interfaces: the interplay of interfacial curvature and nanoparticle–fluid interactions, *Physical Chemistry Chemical Physics*, vol. 19: pp. 3244-3253, 2017.

[17] Bigdeli, M.B., Fasano, M., Cardellini, A., Chiavazzo, E., and Asinari, P., A review on the heat and mass transfer phenomena in nanofluid coolants with special focus on automotive applications, *Renewable and Sustainable Energy Reviews*, vol. 60: pp. 1615-1633, 2016.

[18] Kang, H., Zhang, Y., Yang, M., and Li, L., Molecular dynamics simulation on effect of nanoparticle aggregation on transport properties of a nanofluid, *Journal of Nanotechnology in Engineering and Medicine*, vol. 3: 2, pp. 021001/1-021001/6, 2012.

[19] Eapen, J., Rusconi, R., Piazza, R., and Yip, S., The classical nature of thermal conduction in nanofluids, *Journal of heat transfer*, vol. 132: 10, pp. 102402/1-102402/14, 2010.

[20] Aybar, H.S., Sharifpur, M., Azizian, M.R., Mehrabi, M., and Meyer, J.P., A review of thermal conductivity models for nanofluids, *Heat Transfer Engineering*, vol. 36: 13, pp. 1085-1110, 2015.

[21] Singh, N., Chand, G., and Kanagaraj, S., Investigation of thermal conductivity and viscosity of carbon nanotubes–ethylene glycol nanofluids, *Heat Transfer Engineering*, vol. 33: 9, pp. 821-827, 2012.

[22] Derakhshan, M.M., Akhavan-Behabadi, M.A., and Ghazvini, M., Rheological Characteristics, Pressure Drop, and Skin Friction Coefficient of MWCNT–Oil Nanofluid Flow Inside an Inclined Microfin Tube, *Heat Transfer Engineering*, vol. 36: 17, pp. 1436-1446, 2015.

[23] Hordy, N., Rabilloud, D., Meunier, J.-L., and Coulombe, S., High temperature and long-term stability of carbon nanotube nanofluids for direct absorption solar thermal collectors, *Solar Energy*, vol. 105: pp. 82-90, 2014.

[24] Ding, Y., Alias, H., Wen, D., and Williams, R.A., Heat transfer of aqueous suspensions of carbon nanotubes (CNT nanofluids), *International Journal of Heat and Mass Transfer*, vol. 49: 1, pp. 240-250, 2006.

[25] Abbasi, S.M., Rashidi, A., Nemati, A., and Arzani, K., The effect of functionalisation method on the stability and the thermal conductivity of nanofluid hybrids of carbon nanotubes/gamma alumina, *Ceramics International*, vol. 39: 4, pp. 3885-3891, 2013.

[26] Aravind, S.J., and Ramaprabhu, S., Graphene–multiwalled carbon nanotube-based nanofluids for improved heat dissipation, *RSC Advances*, vol. 3: 13, pp. 4199-4206, 2013.

[27] Khanafer, K., and Vafai, K., A critical synthesis of thermophysical characteristics of nanofluids, *International Journal of Heat and Mass Transfer*, vol. 54: 19, pp. 4410-4428, 2011.
[28] Buongiorno, J., Venerus, D.C., Prabhat, N., McKrell, T., Townsend, J., Christianson, R., Tolmachev, Y.V., Keblinski, P., Hu, L.-w., and Alvarado, J.L., A benchmark study on the thermal conductivity of nanofluids, *Journal of Applied Physics*, vol. 106: 9, pp. 094312/1-094312/14, 2009.
[29] Keblinski, P., Prasher, R., and Eapen, J., Thermal conductance of nanofluids: is the controversy over?, *Journal of Nanoparticle research*, vol. 10: 7, pp. 1089-1097, 2008.
[30] Prasher, R., Evans, W., Meakin, P., Fish, J., Phelan, P., and Keblinski, P., Effect of aggregation on thermal conduction in colloidal nanofluids, *Applied Physics Letters*, vol. 89: 14, pp. 143119/1-143119/3, 2006.
[31] Nan, C.-W., Birringer, R., Clarke, D.R., and Gleiter, H., Effective thermal conductivity of particulate composites with interfacial thermal resistance, *Journal of Applied Physics*, vol. 81: 10, pp. 6692-6699, 1997.
[32] Nwosu, P.N., Meyer, J., and Sharifpur, M., A review and parametric investigation into nanofluid viscosity models, *Journal of Nanotechnology in Engineering and Medicine*, vol. 5: 3, pp. 031008/1-031008/11, 2014.
[33] Einstein, A., Eine neue bestimmung der moleküldimensionen, *Annalen der Physik*, vol. 324: 2, pp. 289-306, 1906.
[34] Mueller, S., Llewellin, E., and Mader, H., The rheology of suspensions of solid particles, in *Proceedings of the Royal Society of London A: Mathematical, Physical and Engineering Sciences*, The Royal Society, pp. 1201-1228, 2009.
[35] Sridhara, V., and Satapathy, L.N., Al2O3-based nanofluids: a review, *Nanoscale research letters*, vol. 6: 1, pp. 1-16, 2011.
[36] Kim, H.J., Lee, S.-H., Lee, J.-H., and Jang, S.P., Effect of particle shape on suspension stability and thermal conductivities of water-based bohemite alumina nanofluids, *Energy*, vol. 90: pp. 1290-1297, 2015.
[37] Ji, Y., Wilson, C., Chen, H.-h., and Ma, H., Particle shape effect on heat transfer performance in an oscillating heat pipe, *Nanoscale research letters*, vol. 6: 1, pp. 1-7, 2011.
[38] Chougule, S.S., and Sahu, S., Comparative Study on Heat Transfer Enhancement of Low Volume Concentration of Al2O3–Water and Carbon Nanotube–Water Nanofluids in Laminar Regime Using Helical Screw Tape Inserts, *Journal of Nanotechnology in Engineering and Medicine*, vol. 4: 4, pp. 040904/1-040904/9, 2013.
[39] Huxtable, S.T., Cahill, D.G., Shenogin, S., Xue, L., Ozisik, R., Barone, P., Usrey, M., Strano, M.S., Siddons, G., Shim, M., and Keblinski, P., Interfacial heat flow in carbon nanotube suspensions, *Nature Materials*, vol. 2: 11, pp. 731-734, 2003.
[40] Timofeeva, E.V., Gavrilov, A.N., McCloskey, J.M., Tolmachev, Y.V., Sprunt, S., Lopatina, L.M., and Selinger, J.V., Thermal conductivity and particle agglomeration in alumina nanofluids: Experiment and theory, *Physical Review E*, vol. 76: 6, pp. 061203/1-061203/16, 2007.

[41] Beck, M.P., Yuan, Y., Warrier, P., and Teja, A.S., The effect of particle size on the thermal conductivity of alumina nanofluids, *Journal of Nanoparticle Research*, vol. 11: 5, pp. 1129-1136, 2009.

[42] Elias, M., Miqdad, M., Mahbubul, I., Saidur, R., Kamalisarvestani, M., Sohel, M., Hepbasli, A., Rahim, N., and Amalina, M., Effect of nanoparticle shape on the heat transfer and thermodynamic performance of a shell and tube heat exchanger, *International Communications in Heat and Mass Transfer*, vol. 44: pp. 93-99, 2013.

[43] Karami, M., Bahabadi, M.A., Delfani, S., and Ghozatloo, A., A new application of carbon nanotubes nanofluid as working fluid of low-temperature direct absorption solar collector, *Solar Energy Materials and Solar Cells*, vol. 121: pp. 114-118, 2014.

[44] Liu, J., Wang, F., Zhang, L., Fang, X., and Zhang, Z., Thermodynamic properties and thermal stability of ionic liquid-based nanofluids containing graphene as advanced heat transfer fluids for medium-to-high-temperature applications, *Renewable Energy*, vol. 63: pp. 519-523, 2014.

[45] Mehrali, M., Sadeghinezhad, E., Latibari, S.T., Kazi, S.N., Mehrali, M., Zubir, M.N.B.M., and Metselaar, H.S.C., Investigation of thermal conductivity and rheological properties of nanofluids containing graphene nanoplatelets, *Nanoscale Research Letters*, vol. 9: 1, pp. 1-12, 2014.

[46] Said, Z., Alim, M., and Janajreh, I., Exergy efficiency analysis of a flat plate solar collector using graphene based nanofluid, in *IOP Conference Series: Materials Science and Engineering*, IOP Publishing, pp. 012015/1-012015/9, 2015.

[47] Said, Z., Saidur, R., Sabiha, M., Rahim, N., and Anisur, M., Thermophysical properties of Single Wall Carbon Nanotubes and its effect on exergy efficiency of a flat plate solar collector, *Solar Energy*, vol. 115: pp. 757-769, 2015.

[48] Tong, Y., Kim, J., and Cho, H., Effects of thermal performance of enclosed-type evacuated U-tube solar collector with multi-walled carbon nanotube/water nanofluid, *Renewable Energy*, vol. 83: pp. 463-473, 2015.

[49] Vakili, M., Hosseinalipour, S., Delfani, S., Khosrojerdi, S., and Karami, M., Experimental investigation of graphene nanoplatelets nanofluid-based volumetric solar collector for domestic hot water systems, *Solar Energy*, vol. 131: pp. 119-130, 2016.

[50] Vincely, D.A., and Natarajan, E., Experimental investigation of the solar FPC performance using graphene oxide nanofluid under forced circulation, *Energy Conversion and Management*, vol. 117: pp. 1-11, 2016.

[51] Yousefi, T., Veisy, F., Shojaeizadeh, E., and Zinadini, S., An experimental investigation on the effect of MWCNT-H 2 O nanofluid on the efficiency of flat-plate solar collectors, *Experimental Thermal and Fluid Science*, vol. 39: pp. 207-212, 2012.

[52] Khullar, V., Tyagi, H., Phelan, P.E., Otanicar, T.P., Singh, H., and Taylor, R.A., Solar energy harvesting using nanofluids-based concentrating solar collector, *Journal of Nanotechnology in Engineering and Medicine*, vol. 3: 3, pp. 031003/1-031003/9, 2012.

[53] Moradi, A., Sani, E., Simonetti, M., Francini, F., Chiavazzo, E., and Asinari, P., Carbon-nanohorn based nanofluids for a direct absorption solar collector for civil

application, *Journal of nanoscience and nanotechnology*, vol. 15: 5, pp. 3488-3495, 2015.

[54] Alaghemandi, M., Algaer, E., Böhm, M.C., and Müller-Plathe, F., The thermal conductivity and thermal rectification of carbon nanotubes studied using reverse non-equilibrium molecular dynamics simulations, *Nanotechnology*, vol. 20: 11, pp. 115704/1-115704/6, 2009.

[55] Han, Z., and Fina, A., Thermal conductivity of carbon nanotubes and their polymer nanocomposites: a review, *Progress in polymer science*, vol. 36: 7, pp. 914-944, 2011.

[56] Shiomi, J., and Maruyama, S., Molecular dynamics of diffusive-ballistic heat conduction in single-walled carbon nanotubes, *Japanese Journal of Applied Physics*, vol. 47: 4R, pp. 2005-2009, 2008.

[57] Balandin, A.A., Thermal properties of graphene and nanostructured carbon materials, *Nature materials*, vol. 10: 8, pp. 569-581, 2011.

[58] Xu, X., Pereira, L.F., Wang, Y., Wu, J., Zhang, K., Zhao, X., Bae, S., Bui, C.T., Xie, R., and Thong, J.T., Length-dependent thermal conductivity in suspended single-layer graphene, *Nature communications*, vol. 5: 3689, pp. 1-6, 2014.

[59] Chien, S.-K., and Yang, Y.-T., The effects of vacancy defects and nitrogen doping on the thermal conductivity of armchair (10, 10) single-wall carbon nanotubes, *Solid State Communications*, vol. 151: 14, pp. 1004-1008, 2011.

[60] Dai-Li, F., Yan-Hui, F., Yang, C., Wei, L., and Xin-Xin, Z., Effects of doping, Stone—Wales and vacancy defects on thermal conductivity of single-wall carbon nanotubes, *Chinese Physics B*, vol. 22: 1, pp. 016501/1-016501/8, 2013.

[61] Park, J., Bifano, M.F., and Prakash, V., Sensitivity of thermal conductivity of carbon nanotubes to defect concentrations and heat-treatment, *Journal of applied physics*, vol. 113: 3, pp. 034312/1-034312/11, 2013.

[62] Hao, F., Fang, D., and Xu, Z., Mechanical and thermal transport properties of graphene with defects, *Applied physics letters*, vol. 99: 4, pp. 041901/1-041901/3, 2011.

[63] Ng, T., Yeo, J., and Liu, Z., A molecular dynamics study of the thermal conductivity of graphene nanoribbons containing dispersed Stone–Thrower–Wales defects, *Carbon*, vol. 50: 13, pp. 4887-4893, 2012.

[64] Yeo, J.J., Liu, Z., and Ng, T.Y., Comparing the effects of dispersed Stone–Thrower–Wales defects and double vacancies on the thermal conductivity of graphene nanoribbons, *Nanotechnology*, vol. 23: 38, pp. 385702/1-385702/7, 2012.

[65] Sevik, C., Sevinçli, H., Cuniberti, G., and Cagın, T., Phonon engineering in carbon nanotubes by controlling defect concentration, *Nano letters*, vol. 11: 11, pp. 4971-4977, 2011.

[66] Zhu, Z., Yang, X., Huang, M., He, Q., Yang, G., and Wang, Z., Mechanisms governing phonon scattering by topological defects in graphene nanoribbons, *Nanotechnology*, vol. 27: 5, pp. 055401/1-055401/7, 2015.

[67] Akilu, S., Sharma, K., Baheta, A.T., and Mamat, R., A review of thermophysical properties of water based composite nanofluids, *Renewable and Sustainable Energy Reviews*, vol. 66: pp. 654-678, 2016.

[68] Ghozatloo, A., Rashidi, A.M., and Shariaty-Niasar, M., Effects of surface modification on the dispersion and thermal conductivity of CNT/water nanofluids, *International Communications in Heat and Mass Transfer*, vol. 54: pp. 1-7, 2014.
[69] Esfe, M.H., Saedodin, S., Mahian, O., and Wongwises, S., Heat transfer characteristics and pressure drop of COOH-functionalized DWCNTs/water nanofluid in turbulent flow at low concentrations, *International Journal of Heat and Mass Transfer*, vol. 73: pp. 186-194, 2014.
[70] Murshed, S.S., and de Castro, C.N., Superior thermal features of carbon nanotubes-based nanofluids–A review, *Renewable and Sustainable Energy Reviews*, vol. 37: pp. 155-167, 2014.
[71] Nasiri, A., Shariaty-Niasar, M., Rashidi, A.M., and Khodafarin, R., Effect of CNT structures on thermal conductivity and stability of nanofluid, *International Journal of heat and Mass transfer*, vol. 55: 5, pp. 1529-1535, 2012.
[72] Sadri, R., Ahmadi, G., Togun, H., Dahari, M., Kazi, S.N., Sadeghinezhad, E., and Zubir, N., An experimental study on thermal conductivity and viscosity of nanofluids containing carbon nanotubes, *Nanoscale research letters*, vol. 9: 1, pp. 1-16, 2014.
[73] Kole, M., and Dey, T., Investigation of thermal conductivity, viscosity, and electrical conductivity of graphene based nanofluids, *Journal of Applied Physics*, vol. 113: 8, pp. 084307/1-084307/8, 2013.
[74] Hone, J., Batlogg, B., Benes, Z., Johnson, A., and Fischer, J., Quantized phonon spectrum of single-wall carbon nanotubes, *Science*, vol. 289: 5485, pp. 1730-1733, 2000.
[75] Pop, E., Varshney, V., and Roy, A.K., Thermal properties of graphene: Fundamentals and applications, *MRS Bulletin*, vol. 37: 12, pp. 1273-1281, 2012.
[76] Pradhan, N., Duan, H., Liang, J., and Iannacchione, G., The specific heat and effective thermal conductivity of composites containing single-wall and multi-wall carbon nanotubes, *Nanotechnology*, vol. 20: 24, pp. 245705/1-245705-8, 2009.
[77] Sandhu, H., and Gangacharyulu, D., An experimental study on stability and some thermophysical properties of multiwalled carbon nanotubes with water–ethylene glycol mixtures, *Particulate Science and Technology*, vol. pp. 1-8, 2016.
[78] Xing, M., Yu, J., and Wang, R., Thermo-physical properties of water-based single-walled carbon nanotube nanofluid as advanced coolant, *Applied Thermal Engineering*, vol. 87: pp. 344-351, 2015.
[79] Bozorg Bigdeli, M., and Fasano, M., Thermal transmittance in graphene based networks for polymer matrix composites, *International Journal of Thermal Sciences* vol. 117C: pp. 98-105, 2017.

Figure Captions List

Fig. 1 Effective thermal conductivity enhancement (λ/λ_0) due to the solvation of Al_2O_3 nanoparticles in water. (a) Sensitivity to nanoparticle shape, at $\phi = 0.01$ and (b) $\phi = 0.02$, as predicted by Equation (1). (c) Nanofluids made of prolate or oblate Al_2O_3 nanoparticles show the largest λ/λ_0 increases ($\phi = 0.02$).

Fig. 2 Schematics of the nanoparticles' geometry for the considered carbon-based nanofluids. (a) Carbon Nanotube. (b) Graphene Nanoplatelet.

Fig. 3 Effect of particle size and defects concentration on its thermal conductivity. (a) Carbon nanotube length vs. thermal conductivity [54]. (b) Concentration of defects vs. thermal conductivity reduction in carbon nanotubes ($\boldsymbol{\lambda_{ref}}$ refers to the pristine one) [65]. (c) Graphene length vs. thermal conductivity [58]. (d) Concentration of defects vs. thermal conductivity reduction in graphene ($\boldsymbol{\lambda_{ref}}$ refers to the pristine one) [66]. Data from the literature (dots) are fitted (dashed lines) by semi-empirical equations, as reported in the text.

Fig. 4 Effective thermal conductivity enhancement ($\boldsymbol{\lambda/\lambda_0}$) due to the solvation of carbon nanoparticles in water, as predicted by Equation (1). (a) Length and defects concentration effects, at $\boldsymbol{\phi = 0.002}$ and (b) $\boldsymbol{\phi = 0.004}$ volume concentration of CNTs in water. (c) Size and defects concentration effects, at $\boldsymbol{\phi = 0.002}$ and (d) $\boldsymbol{\phi = 0.004}$ volume concentration of GNPs in water.

Fig. 5 Effect of nanoparticle shape on the effective viscosity of nanofluids. (a) Einstein coefficient ($\boldsymbol{B}$, see Equation (2)) with different aspect ratios of nanoparticles: numerical results by Mueller *et al.* [34] are best fitted by a double exponential equation (see text). (b) Viscosity enhancement ($\boldsymbol{\mu/\mu_0}$) in carbon-based nanofluids with different volume fraction and aspect ratio of nanoparticles.

Fig. 6 Ratio between Prandtl number of carbon-based nanofluids ($\mathbf{Pr}$) and base fluid ($\mathbf{Pr_0}$). (a) Length and defects concentration effects, at $\boldsymbol{\phi = 0.002}$ and (b) $\boldsymbol{\phi = 0.004}$ volume concentration of CNTs in water. (c) Size and defects concentration effects, at $\boldsymbol{\phi = 0.002}$ and (d) $\boldsymbol{\phi = 0.004}$ volume concentration of GNPs in water. Note that, given the linear correlation between $\boldsymbol{\phi}$ and the main properties of nanofluid (see Equations (1)–(3)), a linear trend of $\mathbf{Pr/Pr_0}$ with $\boldsymbol{\phi}$ is expected.

Figures

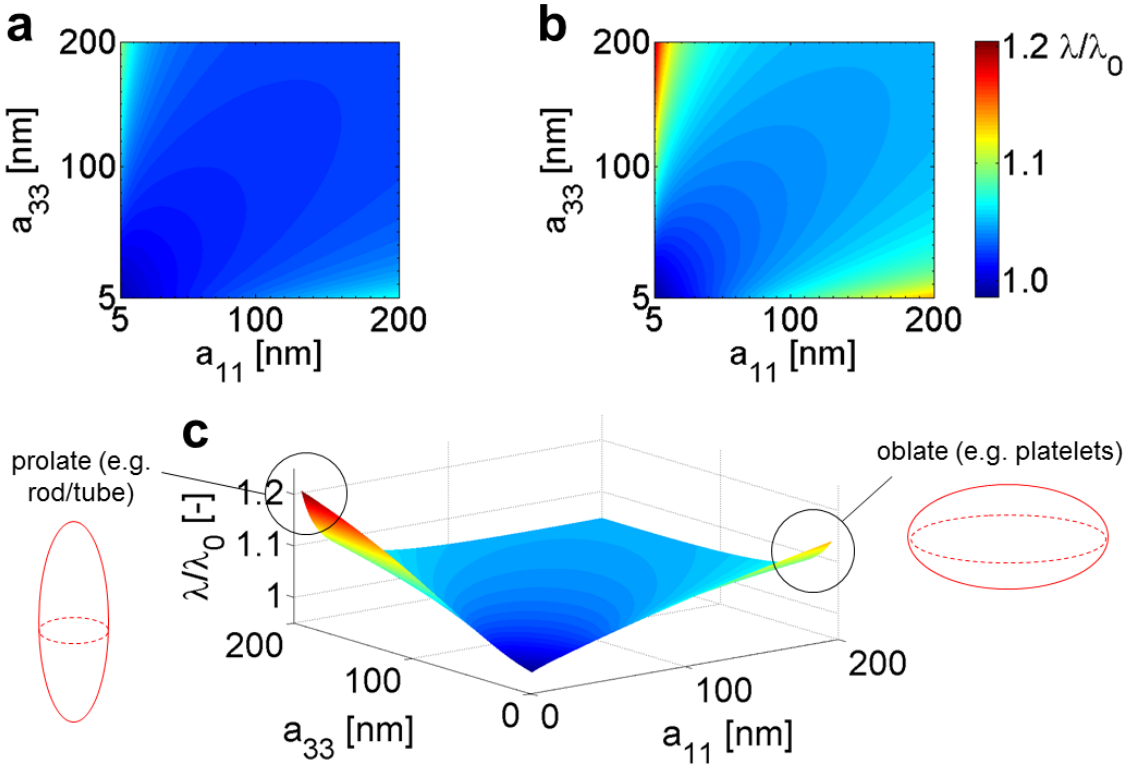

Fig. 1. Effective thermal conductivity enhancement ($\boldsymbol{\lambda/\lambda_0}$) due to the solvation of Al_2O_3 nanoparticles in water. (a) Sensitivity to nanoparticle shape, at $\boldsymbol{\phi = 0.01}$ and (b) $\boldsymbol{\phi = 0.02}$, as predicted by Equation (1). (c) Nanofluids made of prolate or oblate Al_2O_3 nanoparticles show the largest $\boldsymbol{\lambda/\lambda_0}$ increases ($\boldsymbol{\phi = 0.02}$).

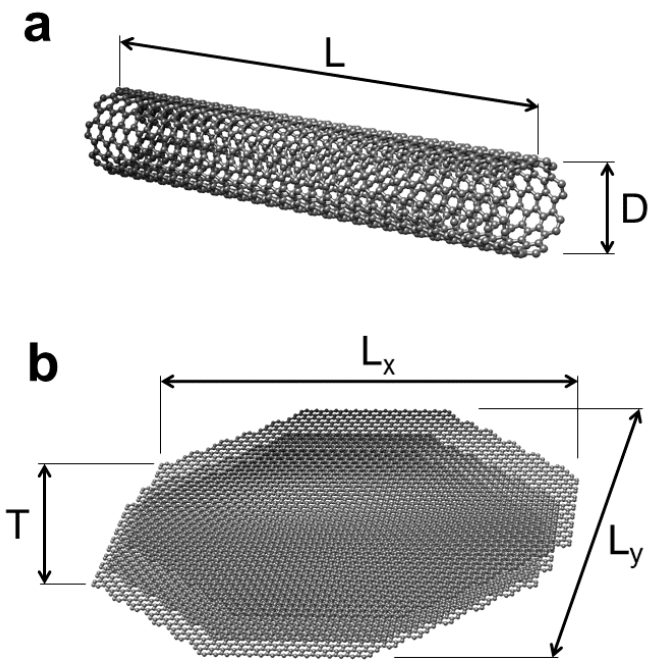

Fig. 2. Schematics of the nanoparticles' geometry for the considered carbon-based nanofluids. (a) Carbon Nanotube. (b) Graphene Nanoplatelet.

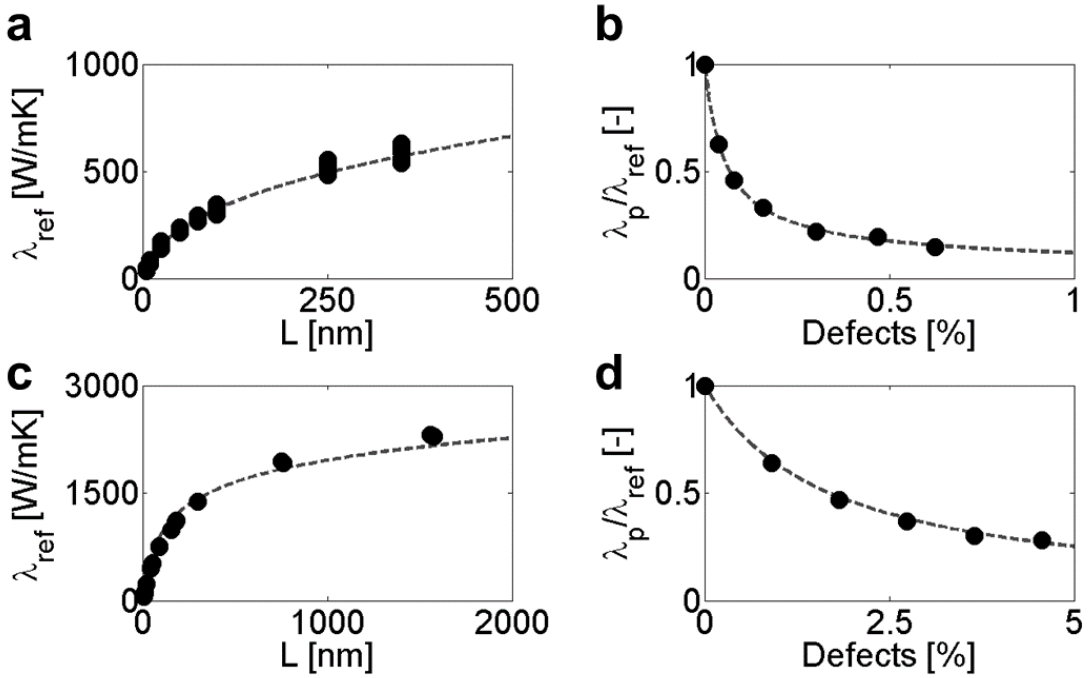

Fig. 3. Effect of particle size and defects concentration on its thermal conductivity. (a) Carbon nanotube length vs. thermal conductivity [54]. (b) Concentration of defects vs. thermal conductivity reduction in carbon nanotubes ($\boldsymbol{\lambda_{ref}}$ refers to the pristine one) [65]. (c) Graphene length vs. thermal conductivity [58]. (d) Concentration of defects vs. thermal conductivity reduction in graphene ($\boldsymbol{\lambda_{ref}}$ refers to the pristine one) [66]. Data from the literature (dots) are fitted (dashed lines) by semi-empirical equations, as reported in the text.

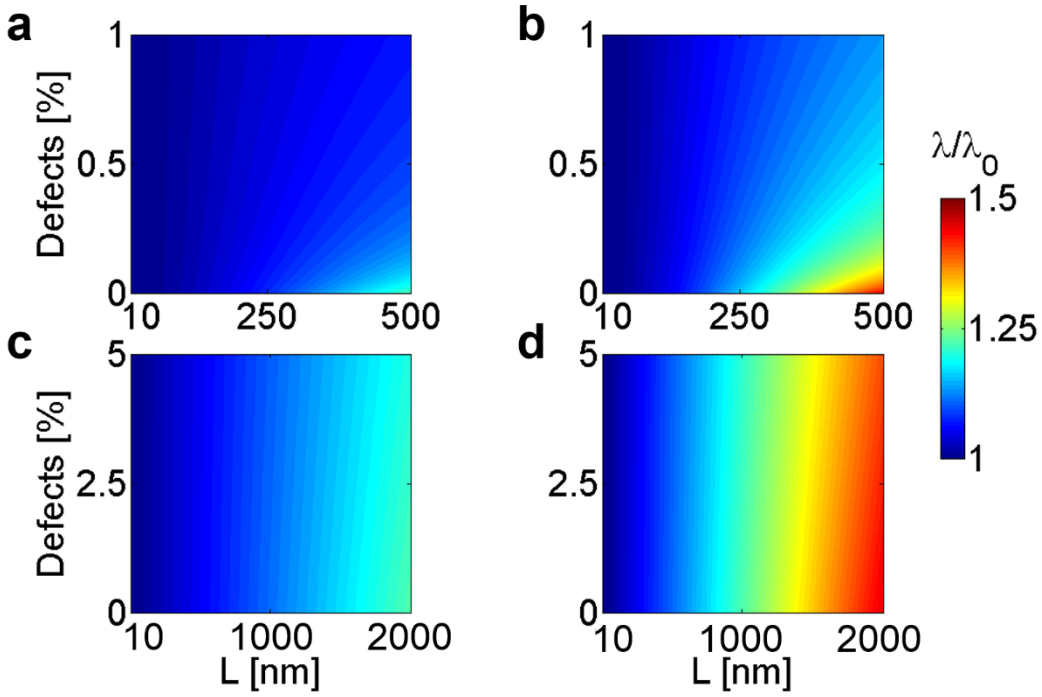

Fig. 4. Effective thermal conductivity enhancement ($\boldsymbol{\lambda/\lambda_0}$) due to the solvation of carbon nanoparticles in water, as predicted by Equation (1). (a) Length and defects concentration effects, at $\boldsymbol{\phi = 0.002}$ and (b) $\boldsymbol{\phi = 0.004}$ volume concentration of CNTs in water. (c) Size and defects concentration effects, at $\boldsymbol{\phi = 0.002}$ and (d) $\boldsymbol{\phi = 0.004}$ volume concentration of GNPs in water.

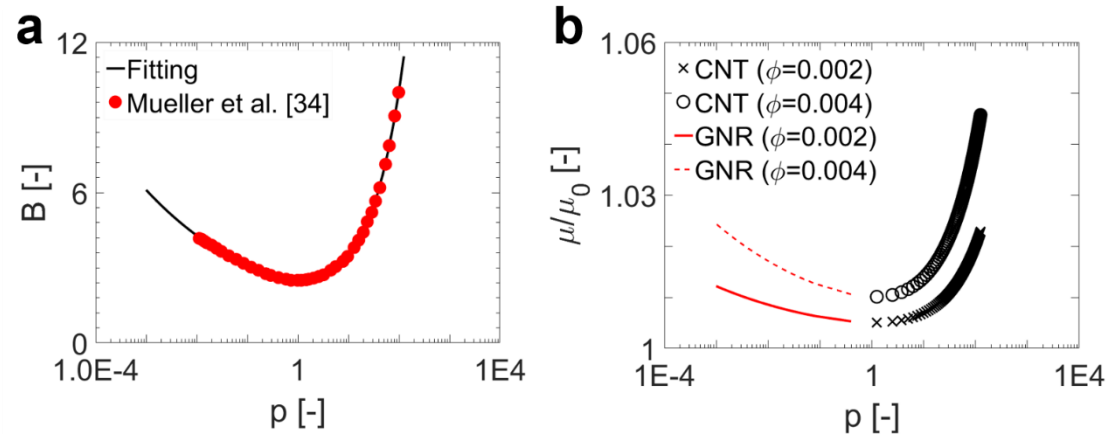

Fig. 5. Effect of nanoparticle shape on the effective viscosity of nanofluids. (a) Einstein coefficient (***B***, see Equation (2)) with different aspect ratios of nanoparticles: numerical results by Mueller *et al.* [34] are best fitted by a double exponential equation (see text). (b) Viscosity enhancement ($\boldsymbol{\mu/\mu_0}$) in carbon-based nanofluids with different volume fraction and aspect ratio of nanoparticles.

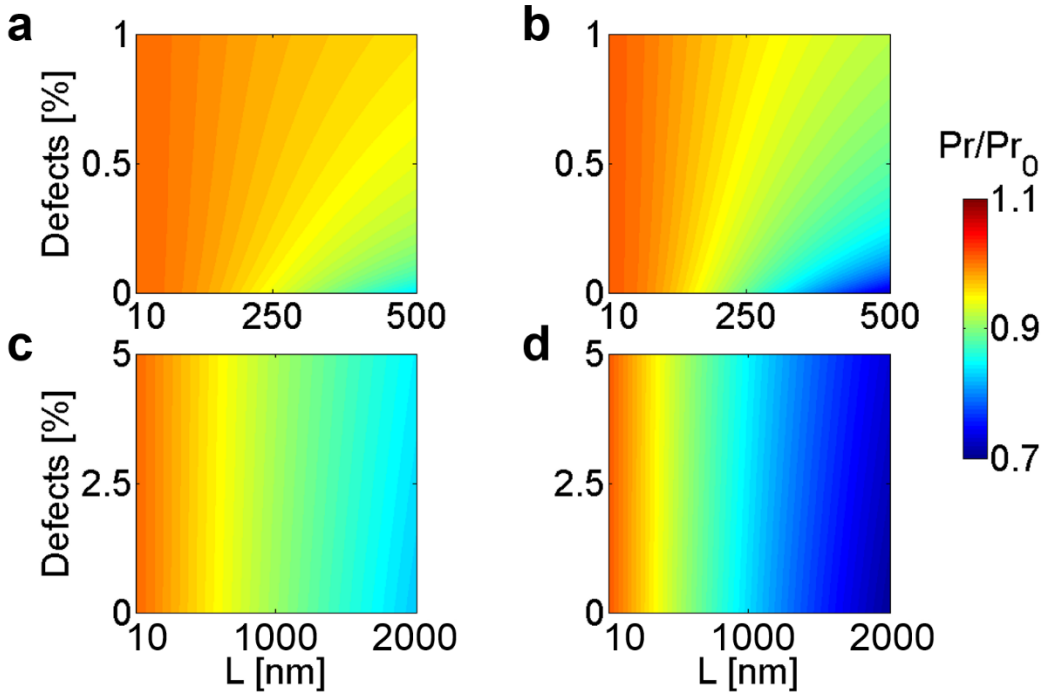

Fig. 6. Ratio between Prandtl number of carbon-based nanofluids (**Pr**) and base fluid ($\mathbf{Pr_0}$). (a) Length and defects concentration effects, at $\boldsymbol{\phi = 0.002}$ and (b) $\boldsymbol{\phi = 0.004}$ volume concentration of CNTs in water. (c) Size and defects concentration effects, at $\boldsymbol{\phi = 0.002}$ and (d) $\boldsymbol{\phi = 0.004}$ volume concentration of GNPs in water. Note that, given the linear correlation between $\boldsymbol{\phi}$ and the main properties of nanofluid (see Equations (1)–(3)), a linear trend of $\mathbf{Pr/Pr_0}$ with $\boldsymbol{\phi}$ is expected.

Biographical Information

Matteo Fasano completed a Ph.D. in Energy Engineering at Politecnico di Torino in 2015. Matteo was visiting research fellow at Houston Methodist Research Institute (01/2013-12/2013, Houston, TX-USA), where he was affiliated to Nanomedicine and Translational Imaging Departments. He was then visiting research fellow at Massachusetts Institute of Technology (07/2014-08/2014, Cambridge, MA-USA), where he carried out a collaborative research at the Department of Mechanical Engineering. During his doctoral studies, he was accepted by Scuola Interpolitecnica di Dottorato for nanotechnology studies, which is a interdisciplinary doctoral school reserved to outstanding doctoral scholars from the three major Italian engineering universities (Politecnico di Milano, Politecnico di Torino, Politecnico di Bari). During his undergraduate studies, he was rewarded by Alta Scuola Politecnica, Accenture and Roberto Rocca scholarships. He is currently postdoctoral fellow at Politecnico di Torino.

Masoud Bozorg Bigdeli is a graduate student at University of Alberta, Dept. of Mechanical Engineering. He received his M.S. in Mechanical Engineering from Politecnico di Torino in 2014; then he worked as research fellow at Politecnico di Torino in 2015. During his studies, he was rewarded by Alta Scuola Politecnica and EDISU Piemonte scholarships. His recent research activities cover heat transfer in nanofluids and nanostructured materials, such as carbon nanotubes and graphene nanoribbons.